

Cold events in thermal-neutron-induced fission of heavy nuclei

A. Díaz-Torres^{1,2,a}, F. Guzmán-Martínez², O. Rodríguez-Hoyos²¹ Institut für Theoretische Physik, Justus-Liebig-Universität Giessen, Heinrich-Buff-Ring 16, D-35392 Giessen, Germany² Instituto Superior de Ciencia y Tecnologías Nucleares, Ave. Salvador Allende y Luaces, P.O.Box. 6163, Havana 10600, Cuba

Received: 29 April 1998 / Revised version: 11 September 1998

Communicated by A. Schäfer

Abstract. An interpretation of the cold fission events in thermal-neutron-induced fission of heavy nuclei is given. The descent from the saddle point is considered as a dynamical process with *reversible coupling* between collective and intrinsic degrees of freedom. The distribution function for the collective variables is expressed as a product of two terms: the *adiabatical* and the *dynamical factors*. A simple model for symmetric fission to study the mass distribution is presented. As example, the calculations are performed for the nucleus ^{264}Fm . Gross features of the cold fission are discussed as well as the dependence of the theoretical mass distribution on the parameters of the model.

PACS. 25.85.-w Fission reactions

1 Introduction

An energy of 20–40 MeV is spent to deform and excite the fragments in the usual fission. These fragments reach ground states by neutron evaporation and gamma ray emission. The remaining part of the Q-value gives the total kinetic energy (TKE) of the fragments. In the cold fission events [1], the TKE value practically exhausts the Q value (neutronless fission). While the component of the cold fission is rare in the U, Np, Pu isotopes [2], it is rather strong in the Fm, Md, No, Cf and other transfermium nuclei [3].

Analogously to the cluster decay the cold spontaneous fission was interpreted [4, 5] as the penetration of a barrier given in the overlapping region by the minimum of the potential energy of the system and in the external region by the interaction of the two fragments in their ground states. The deformations of both fragments seems to be essential for the explanation of the mass and charge distributions in cold fission [6]. For cold fission, only the first two to three rotational levels are populated indicating that the fragmentation process is along the symmetry axis and very slow. In the frame of the interpretation [7] of the cold fission, the total effect of dissipation consists in an enhancement of the quantum tunneling. This conclusion is consistent with our results in a recent paper [8] where we showed that the coupling between collective and intrinsic degrees of freedom gives rise to an enhancement of the state density along the fission path being very much expected beyond the external saddle point with a strong dependence on the shape asymmetry of the fragments.

The aim of this paper is to give an interpretation of the cold fission events in the thermal-neutron-induced fission in which the fission occurs above the barrier. We think that it is possible to try a dynamic image of the cold fission, if a reversible coupling between the intrinsic and collective degrees of freedom is considered. Since we consider the rare cold fission events, the dissipation in our approach is disregarded. Considering the dissipation as a stochastic process, we can assume the descent from the saddle point to scission without dissipation. The reversible coupling induces only mixtures between the intrinsic and collective states, being the average energy available for each subspace constant. The existence of such cold events (cold compact and cold deformed fission) is well established by the experiments, i.e., $^{233}\text{U}(\text{nth},\text{f})$ [9], $^{235}\text{U}(\text{nth},\text{f})$ [10], $^{232}\text{U}(\text{nth},\text{f})$ and $^{239}\text{Pu}(\text{nth},\text{f})$ [11], in the mass and charge yields at very high and very low kinetic energies. In the present work we consider a mechanism to explain the mass distribution of cold events for fission reactions induced by thermal neutrons through a reversible coupling between the mass asymmetry coordinate and the intrinsic degrees of freedom. With the model suitable for symmetric fission, we show a possible reason for the fine structure in the mass yield.

The arrangement of the paper is as follows: In Sect. 2, the theoretical formalism is outlined. In Sect. 3, a model for a heavy nucleus is presented having as a collective mode, a quantum oscillator associated to the mass asymmetry coordinate. The intrinsic degrees of freedom are described as a Fermi gas in the Hartree approach. The fission path will be fixed using the Pashkevich's parametrisation [12]. In Sect. 4, we will explore some of the gross features of the cold fission of a heavy nucleus as well as its theoretical

^a e-mail address:

Alexis.Diaz-Torres@theo-physik.uni-giessen.de

fission mass distribution. For example, the calculation will be carried out for the nucleus ^{264}Fm . This neutron-rich nucleus should be the best cold-fissioning nucleus [13], owing to the strong shell effect of the doubly magic fragments ^{132}Sn . The dependence of the theoretical cold fission mass distribution on the parameters used in our model will be discussed as well the concluding remarks are given in Sect. 5.

2 Theoretical formalism

We take the notation $\{\mathbf{R}\}$ for the set of collective variables and $\{\mathbf{r}'\}$ for the set of the intrinsic ones. The configuration space of the nucleus $\{\mathbf{q}\}$ can be represented as a direct sum of the subspaces of both kinds of variables. The Hilbert space of the nucleus could be generated by the direct product of the state vector basis associated to both kinds of degrees of freedom. Let (τ) and (\mathbf{n}) are the sets of quantum numbers related to the intrinsic and collective degrees of freedom, respectively. The total Hamiltonian of the fissioning nucleus is

$$H_{\text{tot}} = H_i(\mathbf{r}') + H_c(\mathbf{R}) + V_{\text{ic}}(\mathbf{r}', \mathbf{R}), \quad (2.1)$$

where H_i is the intrinsic hamiltonian, H_c the collective one and V_{ic} represents the coupling between both kinds of dynamical variables. The state of the system can be understood as a eigenstate mixture described by the statistical operator 'w' obeying a hamiltonian dynamics. In our stationary system, the probability for the system to occupy a volume 'dq' around 'q' in its configuration space can be expressed with the density-matrix of the ensemble in the energy representation $w(\tau\mathbf{n})$

$$dW_q = \sum_{\tau\mathbf{n}} w(\tau\mathbf{n}) \cdot |\psi_{(\tau\mathbf{n})}(\mathbf{q})|^2 dq, \quad (2.2)$$

where,

$$H_{\text{tot}}\psi_{(\tau\mathbf{n})}(\mathbf{q}) = E_{(\tau\mathbf{n})}\psi_{(\tau\mathbf{n})}(\mathbf{q}). \quad (2.3)$$

If the coupling term V_{ic} is assumed to be weak and the spectrum of ' $H_i + H_c$ ' is not degenerated (for simplification), we can apply the perturbation theory in the first approximation to the problem (2.3) (see [8]). If we assume also that the coupling operator V_{ic} is not diagonal in the basis of adiabatical states $\{|\tau\mathbf{n}\rangle_0 \sim \chi^{(\tau)}(\mathbf{r}') \cdot \varphi^{(\mathbf{n})}(\mathbf{R})\}$ then the average energy of the system is expressed as the sum of the average energy of each one of the subspaces. The functions $\{\chi^{(\tau)}(\mathbf{r}')\}$ and $\{\varphi^{(\mathbf{n})}(\mathbf{R})\}$ are respectively eigenfunctions of H_i and H_c , belonging to the eigenvalues $\{E_i^{(\tau)}\}$ and $\{E_c^{(\mathbf{n})}\}$. So, in this case the coupling induces only mixtures in the intrinsic and collective states described by the statistical operators w_i and w_c . The average energy available for each subspace is conserved while the system is moving in the configuration space. This type of coupling is called *reversible coupling*, because it does not change the entropy of each subspace, and could be presented along the cold fission.

The probability of finding the system in a $d\mathbf{R}$ volume in the space of their collective coordinates for an arbitrary value of the intrinsic coordinates is as follows

$$dW_R = dR \sum_{\tau\mathbf{n}} w(\tau\mathbf{n}) \cdot \int dr' |\psi_{(\tau\mathbf{n})}(\mathbf{q})|^2, \quad (2.4)$$

where

$$\begin{aligned} |\psi_{(\tau\mathbf{n})}(\mathbf{q})|^2 &= |\psi_{(\tau\mathbf{n})}^0(\mathbf{q})|^2 \\ &+ \left| \sum_{\tau'\mathbf{n}'} C(\tau\mathbf{n}; \tau'\mathbf{n}') \cdot \psi_{(\tau'\mathbf{n}')}^0(\mathbf{q}) \right|^2 \\ &+ 2 \text{Re} \left\{ \psi_{(\tau\mathbf{n})}^{0*} \cdot \sum_{\tau'\mathbf{n}'} C(\tau\mathbf{n}; \tau'\mathbf{n}') \cdot \psi_{(\tau'\mathbf{n}')}^0(\mathbf{q}) \right\}, \end{aligned} \quad (2.5)$$

$$C(\tau\mathbf{n}; \tau'\mathbf{n}') = \frac{{}_0\langle \tau\mathbf{n} | V_{\text{ic}} | \tau'\mathbf{n}' \rangle_0}{E_{(\tau\mathbf{n})}^0 - E_{(\tau'\mathbf{n}')}^0}.$$

The contribution of (2.5) to the probability (2.4) is only limited to the first two terms. From the first term in (2.5) we obtain in (2.4)

$$\sum_{\mathbf{n}} \left[\sum_{\tau} w(\tau\mathbf{n}) \cdot \int dr' |\chi^{(\tau)}(\mathbf{r}')|^2 \right] \cdot |\varphi^{(\mathbf{n})}(\mathbf{R})|^2 dR \quad (2.6)$$

The term in brackets represents an average in the ensemble describing the intrinsic states of the systems. For a defined collective state (\mathbf{n}) its quantity is considered proportional to the state density related to the intrinsic degrees of freedom with the coefficient Ξ and the set of orthonormal eigenfunctions $\{\chi^{(\tau)}(\mathbf{r}')\}$

$$\rho_i(\bar{E} - E_c^{(\mathbf{n})}) = \Xi \cdot \sum_{\tau} w(\tau\mathbf{n}). \quad (2.7)$$

where \bar{E} is the total excitation energy. The value of Ξ is obtained from the condition of normalization of the w-matrix

$$\Xi = \sum_{\mathbf{n}} \rho_i(\bar{E} - E_c^{(\mathbf{n})}). \quad (2.8)$$

Taking the contribution of the second term of (2.5) to the probability (2.4) in the first approximation, we obtain

$$\begin{aligned} dW_r &= \Xi^{-1} \sum_{\mathbf{n}} \rho_i(\bar{E} - E_c^{(\mathbf{n})}) \cdot |\varphi^{(\mathbf{n})}(\mathbf{R})|^2 dR \\ &+ \sum_{\mathbf{n}\tau} w(\tau\mathbf{n}) \cdot \sum_{\mathbf{n}'\mathbf{n}''\tau'} C^*(\tau\mathbf{n}; \tau'\mathbf{n}') \cdot C(\tau\mathbf{n}; \tau''\mathbf{n}'') \\ &\cdot \varphi^{(\mathbf{n}')*}(\mathbf{R}) \cdot \varphi^{(\mathbf{n}'')}(\mathbf{R}) dR. \end{aligned} \quad (2.9)$$

For our system where the number of intrinsic variables is quite large, we can use the known Boltzman distribution for the collective density matrix and

$$\rho_i(\bar{E} - E_c^{(\mathbf{n})}) \approx \rho_i(\bar{E}) \cdot e^{-E_c^{(\mathbf{n})}/T}. \quad (2.10)$$

Due to the reversible coupling the excitation energy is redistributed between intrinsic and collective degrees of

freedom. As the result, the cold fragments could appear. Taking into account (2.10) and correspondence of $w(\tau n)$ matrix to the microcanonical ensemble, one can write

$$dW_R = dR \cdot \{Y_R^{adiab.} \cdot Y_R^{dyn.}\}, \quad (2.11)$$

where

$$Y_R^{adiab.} = \frac{\sum_n e^{-E_c^{(n)}/T} \cdot |\varphi(R)|^2}{\sum_n e^{-E_c^{(n)}/T}}, \quad (2.12)$$

$$Y_R^{dyn.} = 1 + \frac{e^{-S(\bar{E})} \cdot \left\{ \sum_n e^{-E_c^{(n)}/T} \right\}}{\sum_n e^{-E_c^{(n)}/T} \cdot |\varphi^{(n)}(R)|^2} \cdot \left\{ \sum_{n,\tau} \sum_{n',n'',\tau'} C^*(\tau n; \tau' n') \cdot C(\tau n; \tau' n'') \cdot \varphi^{(n')*}(R) \cdot \varphi^{(n'')}(R) \right\}, \quad (2.13)$$

being $S(\bar{E})$ the entropy of the system.

An expression similar to (2.12) has been employed by the fragmentation theory [14] to study adiabatically the charge and mass distributions in fission or fusion at low excitation energies. The charge η_z and mass η asymmetries are treated quantum mechanically obeying a Schrödinger's dynamics. The expression (2.13) is a *dynamical factor* modulating the *adiabatical distribution* and it depends on the *reversible coupling* and the excitation energy.

3 Model

Here, we describe a simple model to study the cold fission of a heavy nucleus. The fission path is fixed using the Pashkevich's parametrisation [12] taking the parameters ε , α_1 and α_4 to describe the nuclear shape. The parameter ε reflects the distance between the nascent fragments, α_1 the shape asymmetry and α_4 their deformations. The role of the α_1 and α_4 parameters is relevant in the nuclear shape when the future fragments start to show. The Pashkevich's parametrisation uses Cassinian ovals as figures of the zeroth-order approximation and the deviation from this is represented as a series in Legendre polynomials. This parametrisation describes only axially symmetric nuclear shapes.

We imagine our system like a Fermi gas where nucleons freely move enclosed in a potential well which degenerates gradually into two potential wells during the fission process. As intrinsic variables we consider the set $\{z_i, i = 1, \dots, A\}$ of nucleon z -coordinates related to geometrical center of Cassinian ovals which is situated in the plane that defines the future fragments. Through this plane the exchange of nucleons occurs between two fragments. This collective motion [14] is described by the collective coordinate $\eta = \frac{A_1 - A_2}{A_1 + A_2}$ (A_1 and A_2 are the frag-

ments masses). Under the assumption of a homogeneous mass density, the mass asymmetry coordinate η is reduced to volume asymmetry coordinate $\xi = \frac{V_1 - V_2}{V_1 + V_2}$, where the volumes V_1 and V_2 are defined with a plane through the neck of the fissioning nuclear system. The coordinate ξ is strongly related to α_1 parameter (see [12]). Within the liquid drop model (LDM) one can express the potential in terms of the mass asymmetry coordinate as in [15, 16]

$$V(\eta) = \frac{K_\eta \cdot \eta^2}{2}, \quad (3.1)$$

where K_η is the constant of the potential which is a function of relative distance of the nascent fragments. The time variation of this constant is smooth during the dynamical descent and can be expressed to a good approximation by average value. This constant can be derived, for example, on the basis of the LDM such as in [16], e.g. for the nucleus ^{264}Fm , $K_\eta = 7062 \text{ MeV}$.

In the present paper we disregarded the shell effect. Here, we assume that the collective coordinate η linearly couples to the intrinsic coordinates $\{z_i\}$ as

$$V_{ic} = \gamma \cdot \eta \cdot \sum_{i=1}^A z_i, \quad (3.2)$$

where γ is the strength of the coupling which is taken as a free parameter, constant along the fission process. Once the two future fragments are defined, the momentum distribution of the nucleons at each fragment changes as a result of a continuous changes in the shapes of the fragments. The momentum of the nucleon is quantified as a function of the occupied volume. In the case of cold fission, nucleons must occupy the lowest states of momentum. The difference between the Fermi momenta of the fragments rises with nucleon exchange from one fragment to another. In other words, this nucleon exchange is conditioned by the spatial location of the nucleons, i.e., to the places where the nucleons are moving ($z < 0$ or $z > 0$). This is described by the set of intrinsic variables $\{z_i\}$. With the coupling proposed above we want to express a possible nexus between both kinds of degrees of freedom. It seems clearly that the coupling (3.2) is not diagonal in the harmonic oscillator basis as well as in the plane wave basis as we can see in the Appendix A. This coupling has the properties of a *reversible coupling*.

The mass parameter $m_{\eta\eta}$ of the oscillator was calculated in hydrodynamical models [17] and in the framework of the two-center shell model and cranking model [18]. These calculations yield a dependence of the mass on the distance between nascent fragment and on the mass asymmetry coordinate averaged over all coordinates. For simplicity, we will assume a constant value for this parameter, averaged over all coordinates. Realistic value of the mass $m_{\eta\eta}$ is of the order of 10^{-40} MeV s^2 .

The wave function of Hartree is taken as the intrinsic state vector, e.g. the product of A normalized plane waves in the V volume of the nucleus, which remains constant. The set of internal quantum numbers (τ) is taken as the set of momenta ($\mathbf{p}_1, \dots, \mathbf{p}_A$), which take quasi-continuum

values from $0 - P_F$ in the Fermi sphere if we take the volume of the nucleus large enough. The eigenfunctions and the eigenvalues of the quantum harmonic oscillator's problem are well known [19].

In the following we will calculate the theoretical mass distribution in the framework of this simple model and we will explore some gross features of the cold fission of a heavy nucleus. For example, the calculation will be performed for the nucleus ^{264}Fm .

3.1 Calculation of the adiabatical distribution

The adiabatical distribution was obtained in Sect. 2, and was expressed through the expression (2.12). In the present subsection we only obtain the *adiabatical distribution* of the variable η in the frame of the simple model proposed above. The *adiabatical distribution* is expressed as

$$Y_{adiab.} = \sqrt{\alpha} \cdot e^{-\alpha\eta^2} \cdot \langle A_n^2 \cdot H_n^2(\sqrt{\alpha}\eta) \rangle, \quad (3.1.1)$$

where

$$\langle (\dots) \rangle = \frac{\sum_n e^{-(n+\frac{1}{2})\frac{\hbar\omega}{T}} \cdot (\dots)}{\sum_n e^{-(n+\frac{1}{2})\frac{\hbar\omega}{T}}}, \quad (3.1.2)$$

$$\alpha = \frac{(K_\eta \cdot m\eta\eta)^{1/2}}{\hbar}, \quad (3.1.3)$$

$$\hbar\omega = \hbar \cdot \left(\frac{K_\eta}{m\eta\eta} \right)^{1/2}, \quad (3.1.4)$$

$$A_n^2 = (\sqrt{\pi} \cdot n! \cdot 2^n)^{-1}. \quad (3.1.5)$$

The functions ' H_n ' in (3.1.1) are the Hermite polynomials. Note that the eigenfunctions of the oscillator are normalized in the interval $-\infty$ to ∞ , though the range of definition of our physical coordinate is $-1 \leq \eta \leq 1$. This is possible because in our model the value of α is large enough to make the following approximation,

$$\begin{aligned} \int_{-1}^1 e^{-\alpha\eta^2} \cdot H_n^2(\sqrt{\alpha}\eta) \cdot d\eta &= \frac{1}{\sqrt{\alpha}} \int_{-\sqrt{\alpha}}^{\sqrt{\alpha}} e^{-y^2} \cdot H_n^2(y) \cdot dy \\ &\approx \frac{1}{\sqrt{\alpha}} \int_{-\infty}^{\infty} e^{-y^2} \cdot H_n^2(y) \cdot dy \end{aligned} \quad (3.1.6)$$

3.2 Calculation of the dynamical factor

The *dynamical factor* can be expressed through the expression (2.13). In the frame of the model, being the entropy of the Fermi gas ' $2aT$ ', the *dynamical factor* is expressed as

$$\begin{aligned} F_{dyn.} - 1 &= \frac{e^{-2aT} \cdot e^{\alpha\eta^2} \cdot \sum_{\tau n} \sum_{n', n'', \tau'} C^*(\tau n, \tau' n')}{\sqrt{\alpha} \cdot \langle A_n^2 H_n^2(\sqrt{\alpha}\eta) \rangle} \\ &\cdot C(\tau n, \tau' n'') \cdot \varphi_{n'}^*(\eta) \cdot \varphi_{n''}(\eta) \end{aligned} \quad (3.2.1)$$

where a is the parameter of the level density of Fermi gas model (FGM). For the nucleus ^{264}Fm , $a = 25.68 \text{ MeV}^{-1}$. The wave functions are the known eigenfunctions of the quantum oscillator's problem. Taking the coupling (3.2) into account, we obtain

$$\begin{aligned} &C^*(\tau n, \tau' n') \cdot C(\tau n, \tau' n'') \\ &\approx \frac{\gamma^2}{(\hbar\omega)^2} \left| \left\langle \tau \left| \sum_{i=1}^A z_i \right| \tau' \right\rangle \right|^2 \frac{\langle n|\eta|n' \rangle^* \langle n|\eta|n'' \rangle}{(n-n')(n-n'')}, \end{aligned} \quad (3.2.2)$$

where we assumed that our system contains many particles. The distance between the intrinsic levels is negligible in comparison with the distance between collective vibrational levels. The matrix elements $\langle \tau | z_i | \tau' \rangle$ are calculated in Appendix A. Taking into account (3.2.2) and $\langle n|\eta|n' \rangle \neq 0$ for transitions between closing states of the collective spectrum, the *dynamical factor* of the theoretical mass distribution

$$F_{dyn} - 1 \approx \Pi \cdot e^{-2aT} \cdot I^2(\varepsilon, \alpha_1, \alpha_4) \cdot \left(\frac{\sum_n A_n^2 \phi_n^2(\eta)}{\langle A_n^2 H_n^2(\sqrt{\alpha}\eta) \rangle} \right), \quad (3.2.3)$$

is finally obtained, where,

$$A_n^2 = (\sqrt{\pi} \cdot n! \cdot 2^n)^{-1},$$

$$\phi_n^2(\eta) = [\eta \cdot H_n(\sqrt{\alpha}\eta) \cdot \sqrt{\alpha} - H_{n+1}(\sqrt{\alpha}\eta)]^2,$$

$$\Pi = \frac{\gamma^2}{(\hbar\omega \cdot K_\eta)} \cdot \frac{A^2 P_F^6 R_0^8}{36\pi^2 \hbar^6}.$$

The quantity $I^2(\varepsilon, \alpha_1, \alpha_4)$ expresses the influence of the intrinsic degrees of freedom through the coupling on the theoretical mass distribution. This quantity is proportional to the *dynamical coefficient* of the collective enhancement factor of level density [8]. Note that one of the arguments of this quantity is the shape asymmetry parameter α_1 related to volume or mass asymmetry. In the calculations of the matrix elements $\langle \tau | z_i | \tau' \rangle$ we have assumed a fixed nuclear shape and this could be justified if the collective motion is slower than the motion in the intrinsic degrees of freedom. The dependence of $I^2(\varepsilon, \alpha_1, \alpha_4)$ on the deformation parameter α_4 could permit to study qualitatively the theoretical mass distribution vs. TKE. It is worthwhile to recall that by far the largest fraction of the TKE release in fission is due to the Coulomb repulsion between the nascent fragments at scission. Large and small kinetic energies, therefore, correspond to compact ($\alpha_4 < 0$) and deformed ($\alpha_4 > 0$) scission configurations, respectively.

4 Calculations for the nucleus ^{264}Fm

4.1 Some gross features of the cold fission of a heavy nucleus

In this subsection we will explore some gross features of the cold fission of a heavy nucleus from a statistical point

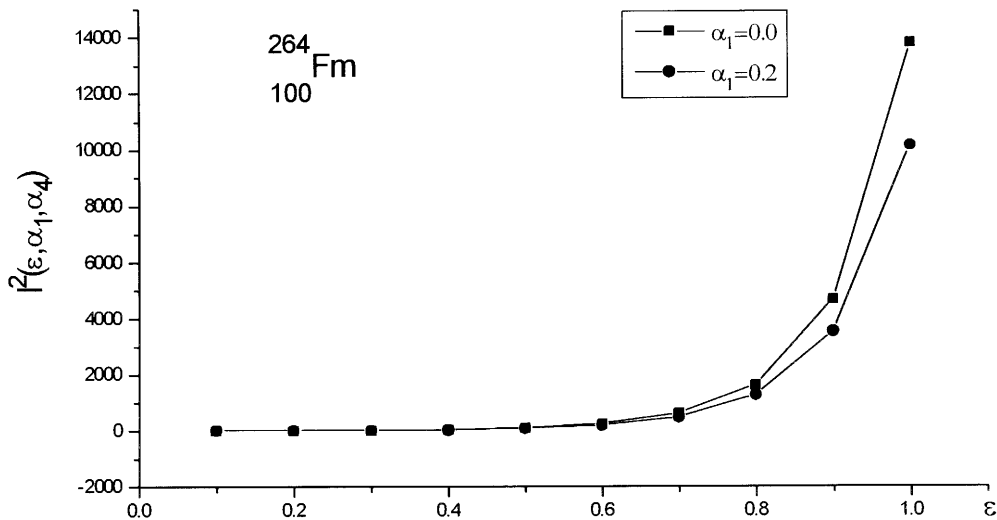


Fig. 1. Dependence of the quantity $I^2(\varepsilon, \alpha_1, \alpha_4)$ on the distance between the fragments measured by “ ε ” parameter of Pashkevich’s parametrisation for two extreme values of the asymmetry measured by “ α_1 ” parameter. The parameter $\alpha_4 = 0$

of view. This could be performed from the study of the *dynamical coefficient* of the total state density [8]. In the cold fission, the *dynamical coefficient* of the total state density is relevant for the final stage of the fission path depending on the nuclear shape by means of the quantity $I^2(\varepsilon, \alpha_1, \alpha_4)$. It is revealed in Fig. 1.

Figures 2a–d show the contour plot of $I^2(\varepsilon, \alpha_1, \alpha_4)$ in the (α_1, α_4) -plane for $\varepsilon = 0.7, 0.8, 0.9$ and 1. If we assume that the cold fission path corresponds to configurations with the greatest values of state density for each distance between the nascent fragments, then these pictures point out a shape transition along the dynamical descent from elongated shapes to compact ones. It can be seen that the state density is greatest for symmetric division ($\alpha_1 = 0$) with the largest variance in α_4 . Near the scission point ($\varepsilon \sim 0.98$), the most probable nuclear configuration corresponds to symmetric fragments ($\alpha_1 = 0$) with spherical shapes (compact shapes) around $\alpha_4 \sim -0.16$. However, because of the large variances of the α_4 values (TKE values) for symmetric mass division, a variety of different modes resulting in deformed as well as spherical shapes could possibly be involved, indicating multimodal fission.

The present discussion from a statistical viewpoint could be an alternative way to study multimodal fission if an unrestricted parametrisation of the nuclear shape is used. There is also the possibility of multimodal fission [20], when a variety of fission channels or pathways are possible for a fissioning nucleus on the same potential energy surface. Microscopic calculations [21] of the potential energy surface of ^{264}Fm minimized for a rather unrestricted parametrisation of the nuclear shape, i.e., Pashkevich’s parametrisation taking into account the higher deformations $\alpha_6, \alpha_8, \alpha_{10}, \dots, \alpha_{20}$, indicate three pre-scission shapes. The first valley corresponds to two symmetric spherical fragments (the ^{132}Sn decay), the second to the standard fission and the third one to a symmetric deformed fragmentation.

4.2 Theoretical mass distribution

In this subsection we study the theoretical mass distribution for $\alpha_4 = 0$. Our intention is not to search for any adjustments, but to study tendencies and the influence of the parameters used by the model, such as: mass parameter, temperature, strength of the coupling and the number of vibrational levels taken into account. Owing to the weakness of the coupling and the low temperature of the system, only the low vibrational levels of the oscillator are taken into account. Calculations are performed taking the first five levels of the oscillator. The mass distribution is normalized to 50%.

Figures 3 and 4 show, respectively, the mass parameter dependence for the *adiabatical distribution* and theoretical mass distribution at scission ($\varepsilon = 0.98$) corresponding to the temperature $T = 0.01$ MeV and a strength of the coupling of $\gamma = 10^{-4}$ MeVfm $^{-1}$. From these figures one can observe that the width of both distributions increases with the decreasing mass parameter. The same behavior is revealed in Fig. 5 but with the increasing temperature. This figure shows the dependence of the *adiabatical distribution* on the temperature for a mass parameter of $m_{\eta\eta} = 10^{-40}$ MeVs 2 .

Figure 6 shows that the theoretical mass distribution is not changed from the external saddle point ($\varepsilon = 0.7$) up to the scission point ($\varepsilon = 0.98$) for a temperature $T = 0.01$ MeV, a mass parameter $m_{\eta\eta} = 10^{-40}$ MeVs 2 and a strength of the coupling of $\gamma = 10^{-4}$ MeVfm $^{-1}$. However, the theoretical mass distribution is changed very much along the dynamical descent for higher temperature $T = 0.17$ MeV and it is revealed in the Fig. 7. This figure shows that asymmetric modes appear in the theoretical mass distribution beyond the external saddle point. It is caused by the increase of the *dynamical factor* through the quantity as we showed in Fig. 1.

In Figs. 6 and 7 one can observe the disappearing asymmetric modes in the theoretical mass distribution

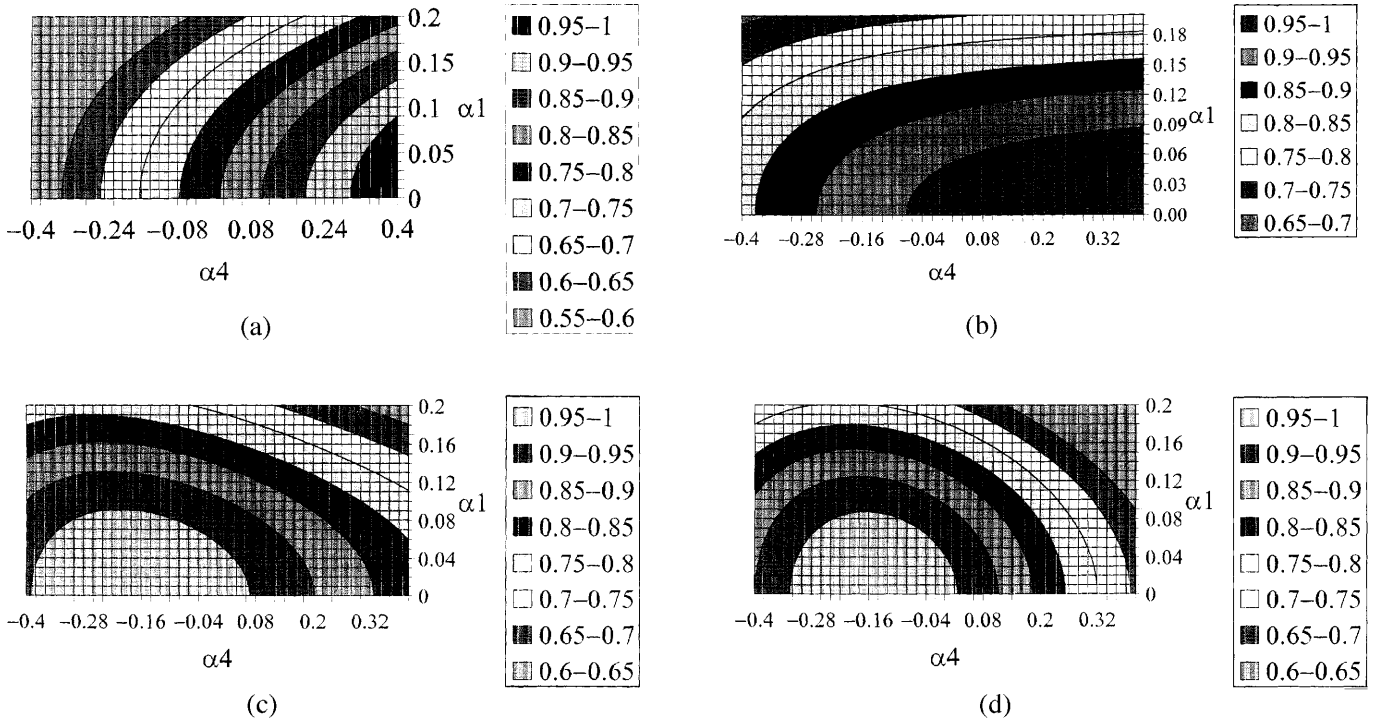


Fig. 2. a–d. The contour plot of $I^2(\epsilon, \alpha_1, \alpha_4)$ with respect to α_1 and α_4 for $\epsilon = 0.7$. The values are normalized between 0 and 1, **b** The same as Figure 2a, but for $\epsilon = 0.8$, **c** The same as Figures 2a, but for $\epsilon = 0.9$, **d** The same as Figures 2a, but for $\epsilon = 1$

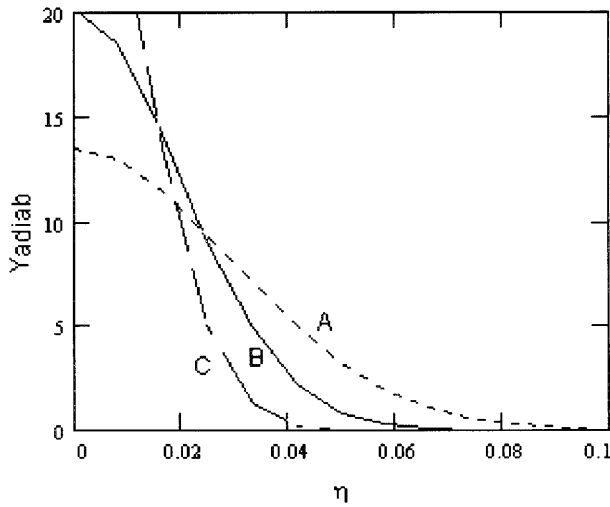


Fig. 3. Dependence of the *adiabatical distribution* on the mass parameter for the temperature $T = 0.01$ MeV. The curves A, B and C are for $m_{\eta\eta} = 0.2, 1$ and 5×10^{-40} MeV s², respectively

with increasing temperature. This effect is due to a decrease of the *dynamical factor* and, thus, the probability $w(\tau\eta)$ for each microcanonical ensemble microstates with the increasing temperature. We could expect the increase of the width of the theoretical mass distribution with increasing temperature.

Figure 8 shows the dependence of the theoretical mass distribution at scission ($\epsilon = 0.98$) point on the strength of the coupling for a temperature $T = 0.01$ MeV and a

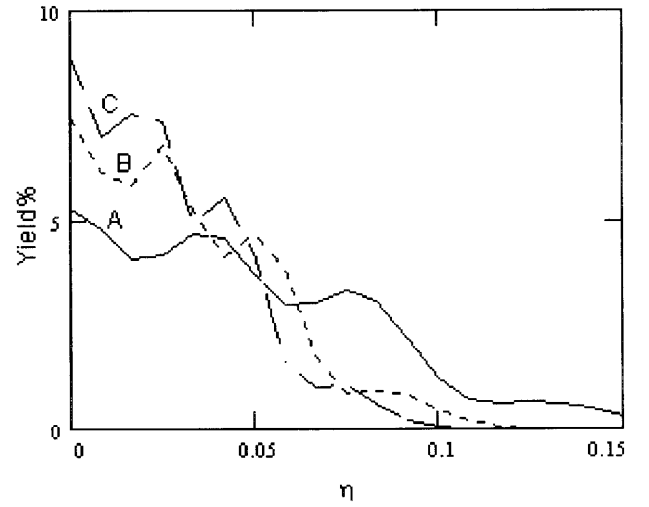


Fig. 4. Dependence of the theoretical mass distribution at scission point ($\epsilon = 0.98$) on the mass parameter for the temperature $T = 0.01$ MeV and a strength of the coupling of $\gamma = 10^{-4}$ MeV fm⁻¹. The curves A, B and C are for $m_{\eta\eta} = 0.2, 1$ and 2×10^{-40} MeV s², respectively. The distribution is normalized to 0,5 for $0 \leq \eta \leq 1$

mass parameter $m_{\eta\eta} = 10^{-40}$ MeVs². In this picture we can observe that the increase of the strength favors the asymmetric modes.

Figure 9 shows the dependence of the theoretical mass distribution at scission ($\epsilon = 0.98$) point on the number of lowest levels of the oscillator taken into account

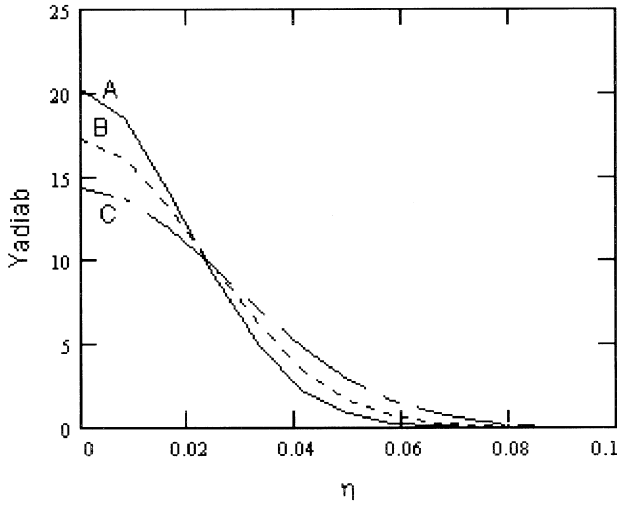


Fig. 5. Dependence of the *adiabatical distribution* on the temperature for the mass parameter $m_{\eta\eta} = 10^{-40} \text{ MeV s}^2$. The curves A, B and C are for $T = 0.01, 3$ and 5 MeV , respectively

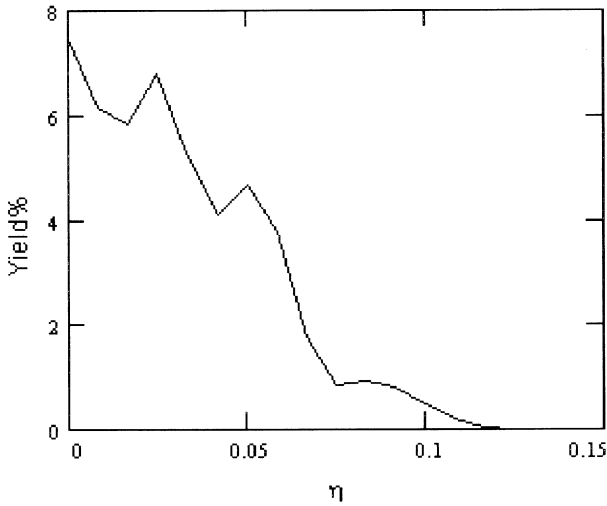


Fig. 6. Dependence of the theoretical mass distribution on the (ϵ parameter for $T = 0.01 \text{ MeV}$, $m_{\eta\eta} = 10^{-40} \text{ MeV s}^2$ and $\gamma = 10^{-4} \text{ MeV fm}^{-1}$. The saddle point distribution ($\epsilon = 0.7$) is equal to the scission point one ($\epsilon = 0.98$). The distribution is normalized to 0,5 for $0 \leq \eta \leq 1$

in the calculations for a temperature $T = 0.01 \text{ MeV}$, $m_{\eta\eta} = 10^{-40} \text{ MeVs}^2$ and a strength of the coupling of $\gamma = 10^{-4} \text{ MeVfm}^{-1}$. It seems that the structures increase when the highly excited vibrational levels of the oscillator are occupied. It is also obtained with the fragmentation theory [14].

Comparing the adiabatical distribution (Figs. 3 and 5) with the theoretical mass distribution shown in Figs. 4, 6–9 it is revealed that the structures are caused by the coupling between the mass asymmetry coordinate and the intrinsic degrees of freedom. The coupling causes transitions between the vibrational levels of the oscillator and its low excited states contribute to the mass distribution. The periodicity of the structures is due to the harmonic

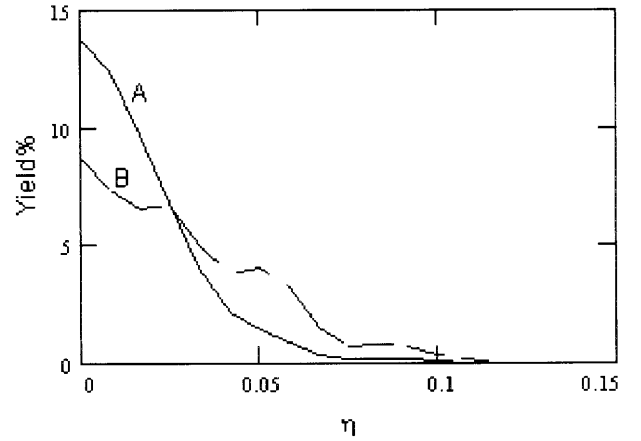


Fig. 7. The same as Figure 6, but for $T = 0.17 \text{ MeV}$. The curves A and B are for $\epsilon = 0.7$ and 0.98 , respectively

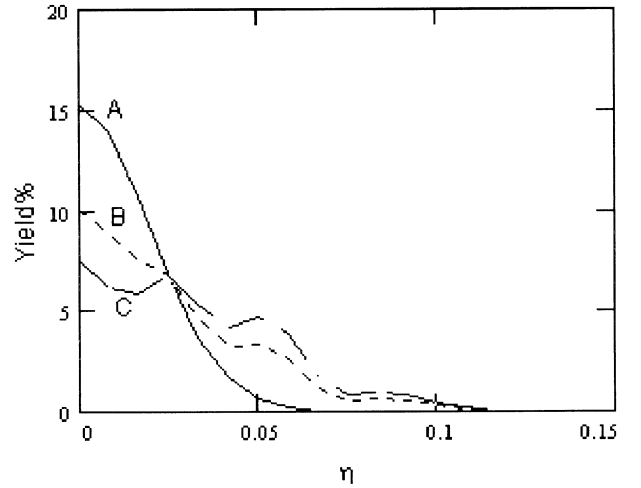


Fig. 8. Dependence of the theoretical mass distribution at scission point ($\epsilon = 0.98$) on the strength of the coupling for $T = 0.01 \text{ MeV}$ and $m_{\eta\eta} = 10^{-40} \text{ MeV s}^2$. The curves A, B and C are for $\gamma = 10^{-8}, 10^{-6}$ and $10^{-4} \text{ MeV fm}^{-1}$, respectively. The distribution is normalized to 0,5 for $0 \leq \eta \leq 1$

oscillator model used to describe the mass asymmetry coordinate, in concrete terms, it is due to the Hermite polynomials in the *dynamical factor*. This periodicity is observed in the experimental mass yields for the cold events and have connection with the odd-even staggerings in its charge yields [10, 11]. Therefore, in general the *dynamical factor* and shell effects are responsible for the structures of the mass distribution of the fission fragments.

5 Concluding remarks

In this paper we presented an interpretation of the cold fission events in the thermal-neutron-induced fission which is considered as a dynamical process with *reversible coupling* between collective and intrinsic degrees of freedom. The *reversible coupling* is defined as nondiagonal in the basis of adiabatical states inducing only mixtures between the

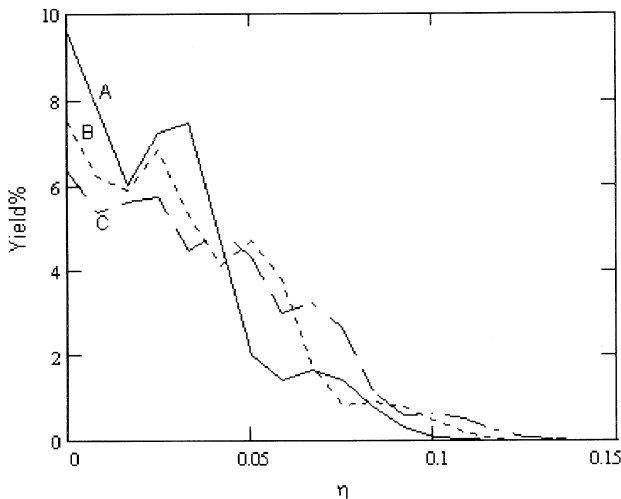


Fig. 9. Dependence of the theoretical mass distribution at scission point ($\varepsilon = 0.98$) on the number N of low vibrational levels taken into account for $T = 0.01$ MeV, $m_{\eta\eta} = 10^{-40}$ MeV s^2 and $\gamma = 10^{-4}$ MeV fm^{-1} . The curves A, B and C are for $N = 3, 5$ and 7 , respectively. The distribution is normalized to 0,5 for $0 \leq \eta \leq 1$

intrinsic and collective states. This type of coupling could be responsible for cold fission. From a quantum statistical point of view a theoretical formalism was presented to describe the distribution of the collective variables. This distribution is expressed as a product of two terms: the *adiabatical distribution* and the *dynamical factor*. The *adiabatical distribution* is similar to the one employed by the fragmentation theory to study adiabatically the charge and mass distributions. The *dynamical factor* includes the *reversible coupling* between collective and intrinsic modes. The model is presented to study the mass distribution of a heavy nucleus having, as a collective mode, a quantum oscillator associated to the mass asymmetry coordinate. For simplicity, we took the Fermi gas model in the Hartree approximation to describe the intrinsic degrees of freedom which are linearly coupled to the mass asymmetry coordinate. The influence of the intrinsic degrees of freedom on the mass distribution is revealed in the *dynamical factor* by a certain quantity proportional to the *dynamical coefficient* of the collective enhancement factor of level density. It permits to explore some gross features of cold fission from a statistical point of view. Near the scission point, the most probable nuclear configuration corresponds to symmetric fragments with compact shapes in agreement with other theoretical predictions. The dynamical effects of the coupling are underlying to the statistical features discussed above. The width of the theoretical mass distribution increase, with decreasing mass parameter and with increasing temperature. The coupling gives rise to asymmetric modes in the theoretical mass distribution. These modes are favored along the dynamical descent but disappear with increasing temperature. This dependence on the temperature is a statistical effect related to the decrease of probability for each microcanonical ensemble of microstates. The theoretical mass distribution is not practi-

cally changed along the dynamical descent for cold nucleus but it is much changed for hot nucleus. The increase of the coupling strength favors the asymmetric modes which also depends on the number of occupied vibrational levels. Due to the weakness of the coupling and the low temperature of the system, only the low vibrational levels of the oscillator could be occupied. We conclude that asymmetric modes could be determined dynamically beyond the saddle point, i.e., running down the barrier, as an effect of the coupling between the mass asymmetry coordinate and the intrinsic degrees of freedom. The extension of our model to the asymmetric fission taking into account the shell effects is in progress.

One of the authors (A.D-T) would like to thank to Professor W. Scheid and Dr. N.V. Antonenko for stimulating discussions and for a careful reading of the manuscript. He also wishes to express gratitude to Professor R.K.Gupta for the fruitful discussions and valuable comments.

This work was supported by The Ministry of Science, Technology and Environment of Cuba and by a grant from the German Academic Exchange Service (DAAD).

6 Appendix A

The matrix elements $\langle \tau | z_i | \tau' \rangle$ are calculated within our simple model. The nondiagonal matrix elements,

$$\langle \dots, \mathbf{p}_i, \dots | z_i | \dots, \mathbf{p}'_i, \dots \rangle = \frac{1}{V} J(|\mathbf{p}_i - \mathbf{p}'_i|) \quad (1A)$$

are not equal to zero, only for $\mathbf{p}_k = \mathbf{p}'_k$ if $k \neq i$.

$$\mathbf{J}(|\mathbf{p}_i - \mathbf{p}'_i|) = \int d^3 \mathbf{r}_i \cdot z_i \cdot \exp \left[\frac{i}{\hbar} (\mathbf{p}_i - \mathbf{p}'_i) \cdot \mathbf{r}_i \right]. \quad (2A)$$

If we assume that the vectors $\Delta \mathbf{p} = \mathbf{p} - \mathbf{p}'$ are in the z -direction, along which the exchange of nucleons occurs, and that its amplitudes are small due to the weakness of coupling, then we can make the following approximation

$$\exp \left(\frac{i}{\hbar} |\Delta \mathbf{p}| z \right) \approx 1 + i \frac{|\Delta \mathbf{p}| z}{\hbar}. \quad (3A)$$

With Pashkevich's parametrisation the integral (2A) is calculated as

$$\mathbf{J}(|\Delta \mathbf{p}|) \approx I_1(\varepsilon, \alpha_1, \alpha_4) + \frac{i}{\hbar} |\Delta \mathbf{p}| \cdot I_2(\varepsilon, \alpha_1, \alpha_4), \quad (4A)$$

where,

$$I_1(\varepsilon, \alpha_1, \alpha_4) = \pi \int_{-1}^1 dx \frac{\partial f_1}{\partial x} \cdot f_1 \cdot G,$$

$$I_2(\varepsilon, \alpha_1, \alpha_4) = \pi \int_{-1}^1 dx \frac{\partial f_1}{\partial x} \cdot f_1^2 \cdot G,$$

$$f_1 = \frac{\bar{z} - z_m}{c},$$

$$G = \left(f_1 + \frac{z_m}{c} \right)^2 - \frac{2}{c^2} [\tilde{R}^2(2x^2 - 1) + \varepsilon R_0^2],$$

$$\bar{z} = \frac{\text{sign}(x)}{\sqrt{2}}.$$

$$\sqrt{\sqrt{(\tilde{R}^4 + 2\varepsilon R_0^2 \tilde{R}^2(2x^2 - 1) + \varepsilon^2 R_0^4 + \tilde{R}^2(2x^2 - 1) + \varepsilon R_0^2)},$$

$$\tilde{R}(x) \approx R_0(1 + \alpha_1 P_1(x) + \alpha_4 P_4(x)),$$

$$R_0 = r_0 \cdot A^{1/3}.$$

The quantities c and z_m determine the volume conservation and the mass center of the system, respectively.

Assuming that our system is large enough, we can do the following

$$\sum_{p,p'} \rightarrow \frac{V^2}{(2\pi\hbar)^6} \int d\mathbf{p} \int d\mathbf{p}'. \quad (5A)$$

The latter permits us to write

$$\sum_{p,p'} \frac{A^2}{V^2} |J(|\Delta\mathbf{p}|)|^2 \approx \frac{A^2 P_F^6 R_0^8}{36\pi^2 \hbar^6} I^2(\varepsilon, \alpha_1, \alpha_4), \quad (6A)$$

where

$$I^2(\varepsilon, \alpha_1, \alpha_4) = \tilde{I}_1^2(\varepsilon, \alpha_1, \alpha_4) + \beta \cdot \tilde{I}_2^2(\varepsilon, \alpha_1, \alpha_4),$$

$$\tilde{I}_1(\varepsilon, \alpha_1, \alpha_4) = \frac{I_1(\varepsilon, \alpha_1, \alpha_4)}{\pi \cdot R_0^4},$$

$$\tilde{I}_2(\varepsilon, \alpha_1, \alpha_4) = \frac{I_2(\varepsilon, \alpha_1, \alpha_4)}{\pi \cdot R_0^5},$$

$$\beta = \frac{6 \cdot P_F^2 \cdot R_0^2}{5 \cdot \hbar^2},$$

$$P_F = \sqrt{2m_0 E_F}.$$

The Fermi energy E_F is assumed as a constant of the order of 39 MeV in all considered energy range.

References

1. D.N. Poenaru, M. Ivascu, W. Greiner, in *Particle Emission from Nuclei*, edited by D.N. Poenaru, M. Ivascu. (Boca Raton, FL: CRC Press 1989), p. 203
2. F. Gönnenwein, in *The Nuclear Fission Process*, edited by C. Wagemans. (Boca Raton, FL: CRC Press 1991), p. 106
3. E.K. Hulet et al., Phys. Rev. Lett. **56**, 313 (1986). D.C. Hoffman, T.M. Hamilton, M.R. Lane, in *Nuclear Decay Modes*, edited by D.N. Poenaru. (Bristol: IOP 1995)
4. W. Greiner, M. Ivascu, D.N. Poenaru, A. Sandulescu, in *Nuclei Far from Stability*, edited by D.A. Bromley. (New York: Plenum Press 1988) p. 641
5. A. Sandulescu, J. Phys. **G15**, 529 (1989)
6. Y.S. Shi, W.J. Swiatecki, Nucl. Phys. **A464**, 205 (1987)
7. E. Stefanescu, W. Scheid, A. Sandulescu, W. Greiner, Phys. Rev. **C53**, 3014 (1996)
8. A. Díaz-Torres, F. Guzmán-Martínez, R. Rodríguez-Guzmán, Z. Phys. **A354**, 409 (1996)
9. W. Schwab, H.-G. Clerc, M. Mutterer, J.P. Theobald and H. Faust, Nucl. Phys. **A577**, 674 (1994)
10. W. Mollenkopf, J. Kaufmann, F. Gönnenwein, P. Geltenbort and A.Oed, J. Phys. **G18**, L203 (1992)
11. J. Kaufmann, W. Mollenkopf, F. Gönnenwein, P. Geltenbort and A. Oed, Z. Phys. **A341**, 319 (1992)
12. V.V. Pashkevich, Nucl. Phys. **A169**, 275 (1971)
13. D.N. Poenaru, J.A. Maruhn, W. Greiner, M. Ivascu, D. Mazilu, R. Gherghescu, Z. Phys. **A328**, 309 (1987). R.A. Gherghescu, D.N. Poenaru, W. Greiner, Z. Phys. **A354**, 367 (1996)
14. J.A. Maruhn, W. Greiner, W. Scheid, in *Heavy ions collisions*. edited by R. Bock. (Amsterdam: North Holland Publ. Comp. 1980)
15. S. Yamaji, W. Scheid, H.J. Fink, W. Greiner, Z. Phys. **A278**, 69 (1976). A. Sandulescu, M. Petrovici, A. Pop, M.S. Popa, J. Hahn, K.H. Ziegenhain, W. Greiner, J.Phys. **G7**, L55 (1981). D.R. Saroha, R. Aroumougame, R.K. Gupta, Phys. Rev. **C27**, 2720 (1983)
16. R.K. Gupta, M. Münchow, A. Sandulescu, W. Scheid, J. Phys. **G10**, 209 (1984)
17. U. Brosa, H.J. Krappe, Z. Phys. **A284**, 65 (1978). H. Kröger, W. Scheid, J. Phys. **G6**, L85 (1980)
18. R.K. Gupta, W. Scheid, W. Greiner, Phys. Rev. Lett. **35**, 353 (1975)
19. L. Landau, E. Lifshitz, in *Course of Theor. Phys. Vol. II*, (Oxford: Pergamon Press 1963)
20. U. Brosa, S. Grossmann, Z. Phys. **A310**, 177 (1983). U. Brosa, S. Grossmann, A. Müller, Phys. Rep. **C197**, 167 (1990)
21. V.V. Pashkevich, Nucl. Phys. **A477**, 1 (1988)